Research article

Shao-Lei Wang, Suo Wang, Xing-Kun Man* and Ren-Min Ma*

Loss and gain in a plasmonic nanolaser

https://doi.org/10.1515/nanoph-2020-0117
Received February 14, 2020; accepted April 3, 2020; published online May 23, 2020

Abstract: Plasmonic nanolasers are a new class of laser devices which amplify surface plasmons instead of photons by stimulated emission. A plasmonic nanolaser cavity can lower the total cavity loss by suppressing radiation loss via the plasmonic field confinement effect. However, laser size miniaturization is inevitably accompanied with increasing total cavity loss. Here we reveal quantitatively the loss and gain in a plasmonic nanolaser. We first obtain gain coefficients at each pump power of a plasmonic nanolaser via analyses of spontaneous emission spectra and lasing emission wavelength shift. We then determine the gain material loss, metallic loss and radiation loss of the plasmonic nanolaser. Last, we provide relationships between quality factor, loss, gain, carrier density and lasing emission wavelength. Our results provide guidance to the cavity and gain material optimization of a plasmonic nanolaser, which can lead to laser devices with ever smaller cavity size, lower power consumption and faster modulation speed.

Keywords: gain; laser miniaturization; loss; plasmonic nanolaser; semiconductor.

1 Introduction

Plasmonic nanolasers are a new class of laser devices with feature size comparable to electronic devices. They offer a new powerful tool for a variety of applications ranging from on-chip optical interconnector, sensing and detection, to biological labeling and tracking [1–7]. In the past decade, plasmonic nanolasers with different configurations and field confinement capabilities have been demonstrated including one dimensional confined devices represented by metal-insulator-metal and metal-insulator-semiconductor gap mode nanolasers [8–15], two dimensional confined devices represented by plasmonic nanowire lasers [16–28], and three dimensional confined devices represented by metallic-nanoparticle lasers and metallic-coated nanolasers [29–50]. Plasmonic nanolaser arrays have also been demonstrated to control the emission directionality and wavelength [51–58].

An essential merit of plasmonic nanolasers is to lower the total cavity loss by suppressing radiation loss via the plasmonic field confinement effect [15, 59, 60]. However, increasing of total cavity loss with cavity size miniaturization is inevitable: pure photonic cavities are plagued by radiation loss, plasmonic cavities by ohmic loss [15, 59]. In this article, we provide a quantitative study of the loss and gain in a plasmonic nanolaser. We first obtain excited carrier concentrations at varied pump intensity from spontaneous emission spectra and lasing emission wavelength shift, which are used to calculate Fermi inversion factors and consequently gain coefficients at each pump intensity. We further determine the gain material loss, metallic loss and radiation loss of the plasmonic nanolaser. Last, we give a correspondence between cavity quality factor, total cavity loss, carrier concentration, emission wavelength and gain material loss.

2 Main text

A plasmonic nanolaser consists of two basic materials of metal and gain materials. Figure 1(a) shows the schematic of a metal-insulator-semiconductor gap mode plasmonic nanolaser, where the electric field is strongly confined at the metal-insulator-semiconductor interface [9, 16]. In contrast to conventional photonic mode lasers where the loss mainly consists of gain material loss due to stimulated absorption and radiation loss, there is an additional metallic loss in plasmonic nanolasers. Figure 1(b) shows the loss and gain of a plasmonic nanolaser in a schematic

***Corresponding authors: Ren-Min Ma**, State Key Lab for Mesoscopic Physics, School of Physics, Peking University, Beijing, China; Frontiers Science Center for Nano-optoelectronics & Collaborative Innovation Center of Quantum Matter, Beijing, China, E-mail: renminma@pku.edu.cn; and **Xing-Kun Man**, Center of Soft Matter Physics and Its Applications, School of Physics, Beihang University, Beijing, China; manxk@buaa.edu.cn. https://orcid.org/0000-0003-4199-5772 (R.-M. Ma)
Shao-Lei Wang: Center of Soft Matter Physics and Its Applications, School of Physics, Beihang University, Beijing, China; State Key Lab for Mesoscopic Physics, School of Physics, Peking University, Beijing, China
Suo Wang: State Key Lab for Mesoscopic Physics, School of Physics, Peking University, Beijing, China

energy band diagram. To achieve lasing state, carriers need to be pumped in the excited energy level to a certain density. However, not all the excited carriers contribute to gain. For semiconductor gain materials, there is a transparency carrier density at which point the excited carriers are used to compensate the gain material loss. The extra excited carriers beyond transparency carrier density are used to compensate the metallic loss and radiation loss. Note that the total carrier number at lasing state can be used to calculate the threshold pump power [61].

We first focus on a room-temperature plasmonic nanolaser constructed by a CdSe nanosquare on top of Au film separated by 5 nm MgF_2 as we reported previously [62]. The nanolaser is optically pumped by a nanosecond pump laser at 532 nm (repetition rate: 1 kHz, pulse length: 4.5 ns). Figure 2(a) shows emission spectra evolution with the increase of the pump power. There is a clear resonant peak blue shift below and around lasing threshold which results from the decrease of the refractive index due to the free-carrier dispersion. The blue shift saturates above the lasing threshold due to the gain clamping. The emission wavelength (λ) is related to the real part of the refractive index by $n_r L = m\lambda$, where L is the optical round-trip path inside the cavity and m is the order of the mode. Based on the Drude–Lorentz equation, we can get the density of electrons (N_e) and holes (N_h) to the change of refractive index [63]:

$$\Delta n_r = \frac{-e^2\lambda_0^2}{8\pi^2 c^2 \varepsilon_0 n_r}\left(\frac{\Delta N_e}{m_{ce}^*} + \frac{\Delta N_h}{m_{ch}^*}\right) \quad (1)$$

where e is the electronic charge, λ_O is the peak emission wavelength, c is the light speed in vacuum, ε_0 is the permittivity of free space, $m_{ce}^* = 0.13 \quad m_0 \quad (m_{ch}^* = 0.45 \quad m_0)$ is the effective mass of electrons (holes) of CdSe, m_0 is free electron mass. Since the photo-excited electrons and holes are dominant carriers in the laser cavity, we can assume that ΔN_e equals to ΔN_h. Based on Equation (1), we can obtain the change of carrier density under varied pump powers.

We then calculate carrier concentrations at pump powers well below threshold by fitting spontaneous emission spectra. For a given carrier density, quasi-Fermi levels are determined for photon excited electrons and holes, which can be used to obtain Fermi inversion factor and then the gain spectrum. The gain spectrum is related to the spontaneous emission spectrum via Einstein coefficient relations on spontaneous emission and stimulated emission. We utilize the relationship between the gain spectrum $g(\lambda)$ and the spontaneous emission spectrum $P_{sp}(\lambda)$ [64]:

$$g(\lambda) = A\lambda^5\left[1 - \exp\left(\frac{hc/\lambda - \Delta F}{k_B T}\right)\right]P_{sp}(\lambda) \quad (2)$$

where $\Delta F = E_{Fc} - E_{Fv}$ is the difference of the conduction and valence band quasi-Fermi levels.A is a constant related to volume of the gain material, the ratio of the final measured spontaneous emission power to the total spontaneous emission power and also the confinement factor; hc/λ is the energy of the one photon, k_B is the Boltzmann constant, T is the room temperature of ~300 K. Figure 2(b) shows the fitted results of the spontaneous emission spectra under pump power of 15 kW cm^{-2} and 30 kW cm^{-2} which give carrier densities of ~1.2 × 10^{18} cm^{-3} and ~2.2 × 10^{18} cm^{-3} respectively. Based on above calculations, we obtain the carrier densities at all measured pump

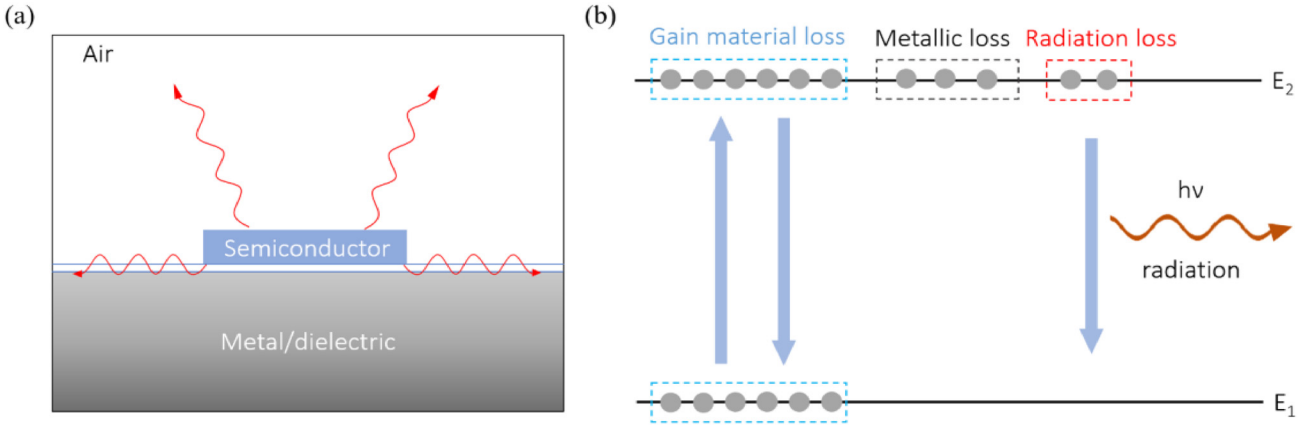

Figure 1: Schematic of loss and gain in a plasmonic nanolaser. (a) Schematic of a plasmonic nanolaser consisting of a semiconductor gain material on top of a metal/dielectric substrate. Red wavy lines represent free space radiation and surface plasmon polariton radiation. (b) Loss and gain of a plasmonic nanolaser in a schematic energy band diagram. To achieve lasing state, carriers need to be pumped in the excited energy level to a certain density, the radiation of which compensates gain material absorption loss, metallic loss and radiation loss.

powers as shown in Figure 2(c). We can see that carrier density increases with the pump power and gets saturated above lasing threshold.

Extracted carrier densities give the maximum gain coefficients in the gain spectra at each pump power as shown in Figure 3(a), which can be used to determine the gain material loss, metallic loss and radiation loss of the plasmonic nanolaser. First, at the full lasing state, the gain coefficient saturates at ~15,100 cm^{-1} which approximately equals to the summation of metallic loss and radiation loss. The wavelength of the lasing peak is at 707.0 nm. The gain material loss at this wavelength is ~29,400 cm^{-1} as shown in Figure 3(b). Second, around the lasing threshold where the cavity resonance just starts to supply feedback, the gain from CdSe approximately just compensates the metallic loss. This condition can be recognized as the resonant peak emerging in the spontaneous emission background, which is at ~109 kW cm^{-2} corresponding to a gain coefficient of 12,600 cm^{-1}. Thereby we can get the metallic loss and radiation loss to be 12,600 cm^{-1} and 2500 cm^{-1} respectively, which is consistent with our full wave simulation result. Estimated from the quality factors of the cavity with and without ohmic loss, the simulation gives a metallic loss and radiation loss to be ~12,500 cm^{-1} and ~2600 cm^{-1} respectively.

Quality factor characterizes the photon loss rate of a cavity. An unambiguously definition of the laser threshold can be described as the condition in which the rates of spontaneous and stimulated emission into the laser mode are equal, because the stimulated emission needs to dominate in the lasing state. According to Einstein coefficient relations on spontaneous emission and stimulated emission [65], this condition requires a lasing mode containing one photon to reach the threshold [61]. So to

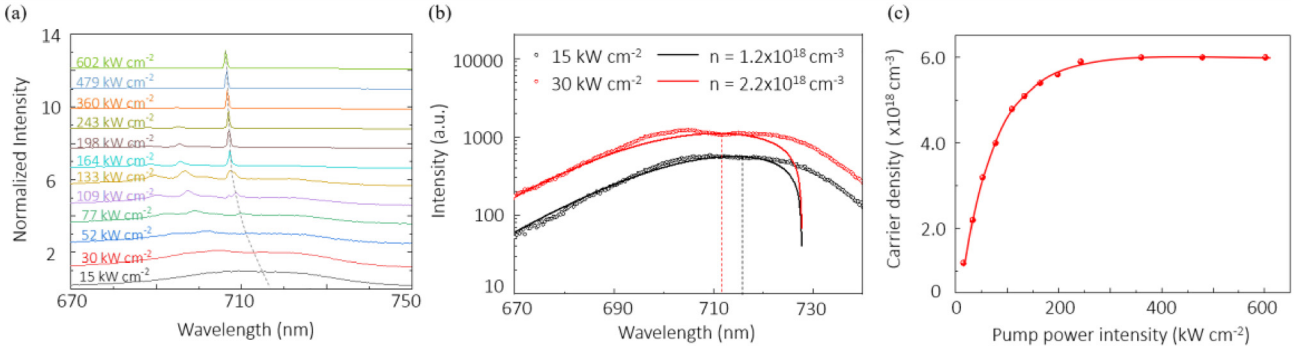

Figure 2: Carrier densities in a plasmonic nanolaser at varied pump power. (a) Emission spectra evolution with the increase of the pump power. The dash curve indicates the resonance peak shift of the lasing mode; (b) Fitting of spontaneous emission spectrum to obtain gain spectrum at pump power well below threshold. Circles: experimental spectra. Lines: fitting curves. (c) Extracted carrier densities at varied pump power.

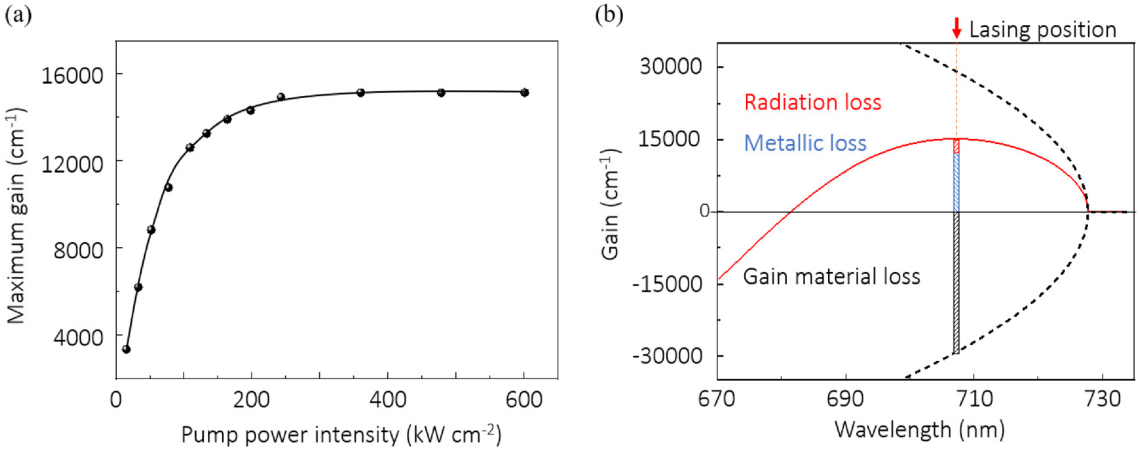

Figure 3: Gain and loss compensation in the plasmonic nanolaser. (a) Extracted maximum gain coefficients at varied pump power. (b) Gain spectrum at full lasing state. The maximum gain in the gain spectrum approximately equals to the sum of the metallic loss and radiation loss.

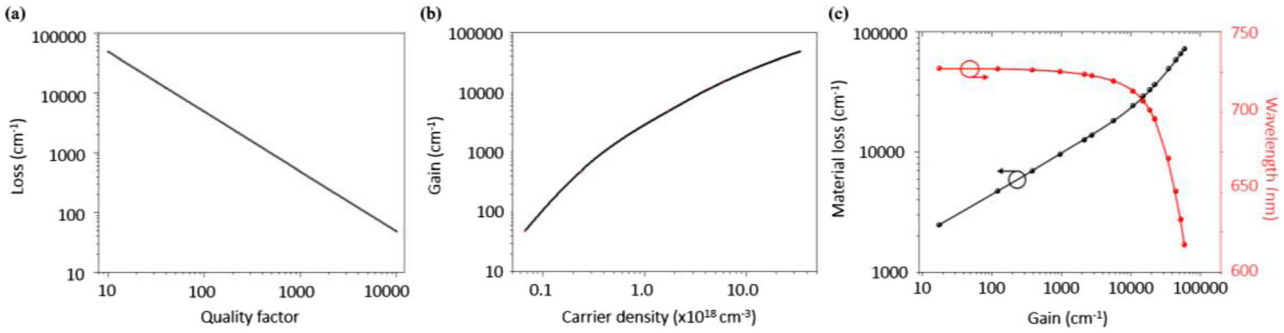

Figure 4: The relationships between quality factor, loss, gain, carrier density and lasing emission wavelength. (a) Relationship of the quality factor and the loss coefficient. (b) Relationship of the gain coefficient and carrier density of CdSe. (c) Gain coefficient versus the corresponding wavelength and gain material loss for CdSe.

optimize the quality factor is essential to lower the threshold of a laser. The loss coefficient of a cavity can be calculated by $\frac{\omega}{\Gamma Q v_g}$, where ω is the resonant frequency, Γ is the confinement factor, Q is the quality factor and v_g is the group velocity of the cavity mode. Figure 4(a) shows the relationship of the quality factor and the loss coefficient, which is calculated based on the condition of $\omega = 2.69 \times 10^{14}$ rad/s, $\Gamma = 0.7$, $v_g = 7.94 \times 10^7$ m/s.

Figure 4(b) shows the carrier densities to acquire varied gain coefficient for CdSe. As well known, a smaller quality factor means a larger loss coefficient and thereby a higher gain coefficient to compensate for lasing. However, for a given gain material, the highest gain is limited by the catastrophic damage threshold of the material due to thermal effect which becomes severer with increasing pump power. With the increase of the carrier density, a gain material can give a higher gain coefficient at a shorter wavelength in the gain spectrum due to enlarged separation of quasi-Fermi levels of the conduction and valence band. Figure 4(c) shows the calculated gain coefficient versus the corresponding wavelength for CdSe. A higher required gain for lasing means a higher gain material loss as also shown in Figure 4(c).

3 Conclusion and discussion

In summary, we have revealed the loss and gain in a plasmonic nanolaser. We obtained gain coefficients at each pump power of a plasmonic nanolaser and determined its gain material loss, metallic loss and radiation loss. We further provided relationships between quality factor, loss, gain, carrier density and lasing emission wavelength. While a plasmonic nanolaser cavity can lower the total cavity loss by suppressing radiation loss via the plasmonic field confinement effect, its cavity size miniaturization is also inevitably accompanied with increasing total cavity loss. Searching materials with higher optical gain and designing plasmonic nanocavities with lower cavity loss are crucial for the development of plasmonic nanolasers. In the design of plasmonic nanolasers, optimization of metallic loss and radiation loss attracts dominant attention. While the minimization of the two will benefit the laser performance, we can see that the gain material loss is always larger than the summation of them as the carriers are far from fully inversion for semiconductor gain materials at room temperature. For a small laser cavity with large free spectral range, the design of the lasing resonance wavelength of the cavity is also essential to lower the total cavity loss, because the gain material loss is strongly wavelength dependent. Our work gives guidance to the cavity and gain material optimization of a plasmonic nanolaser, which can lead to laser device with ever smaller cavity size, lower power consumption and faster modulation speed.

Acknowledgements: This work is supported by NSFC under project Nos. 11774014, 91950115, 11574012 and 61521004, Beijing Natural Science Foundation (Z180011) and the National Key R&D Programme of China (2018YFA0704401).

References

[1] D. J. Bergman, M. I. Stockman, "Surface plasmon amplification by stimulated emission of radiation: quantum generation of coherent surface plasmons in nanosystems," *Phys. Rev. Lett.*, vol. 90, Art no. 027402, 2003, https://doi.org/10.1103/physrevlett.90.027402.

[2] P. Berini, I. De Leon, "Surface plasmon–polariton amplifiers and lasers," *Nat. Photon.*, vol. 6, pp. 16–24, 2012, https://doi.org/10.1038/nphoton.2011.285.

[3] R. M. Ma, R. F. Oulton, V. J. Sorger, X. Zhang, "Plasmon lasers: coherent light source at molecular scales," *Laser Photon. Rev.*, vol. 7, pp. 1–21, 2013, https://doi.org/10.1002/lpor.201100040.

[4] M. T. Hill, M. C. Gather, "Advances in small lasers," *Nat. Photon.*, vol. 8, pp. 908–918, 2014, https://doi.org/10.1038/nphoton.2014.239.
[5] S. Gwo, C. K. Shih, "Semiconductor plasmonic nanolasers: current status and perspectives," *Rep. Prog. Phys.*, vol. 79, Art no. 086501, 2016, https://doi.org/10.1088/0034-4885/79/8/086501.
[6] D. Wang, W. Wang, M. P. Knudson, G. C. Schatz, T. W. Odom, "Structural engineering in plasmon nanolasers," *Chem. Rev.*, vol. 118, pp. 2865–2881, 2018, https://doi.org/10.1021/acs.chemrev.7b00424.
[7] X. Liu, P. Xu, Y. Wu, et al., "Control, optimization and measurement of parameters of semiconductor nanowires lasers," *Nano Energy*, vol. 14, pp. 340–354, 2015, https://doi.org/10.1016/j.nanoen.2014.11.044.
[8] M. T. Hill, M. Marell, E. S. P. Leong, et al., "Lasing in metal-insulator-metal sub-wavelength plasmonic waveguides," *Opt. Express*, vol. 17, pp. 11107–11112, 2009, https://doi.org/10.1364/oe.17.011107.
[9] R. M. Ma, R. F. Oulton, V. J. Sorger, G. Bartal, X. Zhang, "Room-temperature sub-diffraction-limited plasmon laser by total internal reflection," *Nat. Mater.*, vol. 10, pp. 110–113, 2011, https://doi.org/10.1038/nmat2919.
[10] R. M. Ma, S Ota, Y. M. Li, S. Yang, X. Zhang, "Explosives detection in a lasing plasmon nanocavity," *Nat. Nanotechnol.*, vol. 9, pp. 600–604, 2014, https://doi.org/10.1038/nnano.2014.135.
[11] X. Y. Wang, Y. L. Wang, S. Wang, et al., "Lasing enhanced surface plasmon resonance sensing," *Nanophotonics*, vol. 5, pp. 52–58, 2016, https://doi.org/10.1515/nanoph-2016-0006.
[12] Guo C. C., Xiao J. L., Yang Y. D., Zhu Z. H., Huang Y. Z., "Lasing characteristics of wavelength-scale aluminum/silica coated square cavity," *IEEE Photon. Technol. Lett.*, 28, 217–220, 2016, https://doi.org/10.1109/LPT.2015.2492605.
[13] H. Z. Chen, J. Q. Hu, S. Wang, et al., "Imaging the dark emission of spasers," *Sci. Adv.* 2017, vol. 3, Art no. e1601962, https://doi.org/10.1126/sciadv.1601962.
[14] S. Wang, B. Li, X. Y. Wang, et al., "High-yield plasmonic nanolasers with superior stability for sensing in aqueous solution," *ACS Photonics*, vol. 4, pp. 1355–1360, 2017, https://doi.org/10.1021/acsphotonics.7b00438.
[15] S. Wang, X. Y. Wang, B. Li, et al., "Unusual scaling laws for plasmonic nanolasers beyond the diffraction limit," *Nat. Commun.*, vol. 8, pp. 1889, 2017, https://doi.org/10.1038/s41467-017-01662-6.
[16] R. F. Oulton, V. J. Sorger, T. Zentgraf, et al., "Plasmon lasers at deep subwavelength scale," *Nature*, vol. 461, pp. 629–632, 2009, https://doi.org/10.1038/Nature08364.
[17] Y. J. Lu, J. Kim, H. Y. Chen, et al., "Plasmonic nanolaser using epitaxially grown silver film," *Science*, vol. 337, pp. 450–453, 2012, https://doi.org/10.1126/science.1223504.
[18] X. Liu, Q. Zhang, J. N. Yip, Q. Xiong, T. C. Sum, "Wavelength tunable single nanowire lasers based on surface plasmon polariton enhanced Burstein–Moss effect," *Nano Lett.*, vol. 13, pp. 5336–5343, 2013, https://doi.org/10.1021/nl402836x.
[19] T. Sidiropoulos, R. Röder, S. Geburt, et al., "Ultrafast plasmonic nanowire lasers near the surface plasmon frequency," *Nat. Phys.*, vol. 10, pp. 870–876, 2014, https://doi.org/10.1038/nphys3103.
[20] Q. Zhang, G. Li, X. Liu, et al., "A room temperature low-threshold ultraviolet plasmonic nanolaser," *Nat. Commun.*, 2014, vol. 5, pp. 4953, https://doi.org/10.1038/ncomms5953.
[21] Y. J. Lu, C. Y. Wang, J. Kim, et al., "All-color plasmonic nanolasers with ultralow thresholds: autotuning mechanism for single-mode lasing," *Nano Lett*, 2014, vol. 14, pp. 4381–4388, https://doi.org/10.1021/nl501273u.
[22] J. Ho, J. Tatebayashi, S. Sergent, C. F. Fong, S. Iwamoto, Y. Arakawa, "Low-threshold near-infrared GaAs–AlGaAs core–shell nanowire plasmon laser," *ACS Photonics*, vol. 2, pp. 165–171, 2015, https://doi.org/10.1021/ph5003945.
[23] J. Ho, J. Tatebayashi, S. Sergent, et al., "A nanowire-based plasmonic quantum dot laser," *Nano Lett.*, vol. 16, pp. 2845–2850, 2016, https://doi.org/10.1021/acs.nanolett.6b00706.
[24] Y. H. Chou, Y. M. Wu, K. B. Hong, et al., "High-operation-temperature plasmonic nanolasers on single-crystalline aluminum," *Nano Lett.*, vol. 16, pp. 3179–3186, 2016, https://doi.org/10.1021/acs.nanolett.6b00537.
[25] H. Yu, T. Sidiropoulos, W. Liu, et al., "Influence of silver film quality on the threshold of plasmonic nanowire lasers," *Adv Opt Mater*, vol. 5, Art no. 1600856, 2017, https://doi.org/10.1002/adom.201600856.
[26] C. J. Lee, H. Yeh, F. Cheng, et al., "Low-threshold plasmonic lasers on a single-crystalline epitaxial silver platform at telecom wavelength," *ACS Photonics*, vol. 4, pp. 1431–1439, 2017, https://doi.org/10.1021/acsphotonics.7b00184.
[27] S. J. P. Kress, J. Cui, P. Rohner, et al., "A customizable class of colloidal-quantum-dot spasers and plasmonic amplifiers," *Sci. Adv*, vol. 3, Art no. e1700688, 2017, https://doi.org/10.1126/sciadv.1700688.
[28] H. Z. Chen, S. Wang, R. M. Ma, "Characterization of Plasmonic Nanolasers in Spatial, Momentum, and Frequency Spaces," *IEEE J. Quant. Electron.*, vol. 54, Art no. 7200307, 2018, https://doi.org/10.1109/jqe.2018.2853258.
[29] M. T. Hill, Y. S. Oei, B. Smalbrugge, et al., "Lasing in metallic-coated nanocavities," *Nat. Photon*, vol. 1, pp. 589–594, 2007, https://doi.org/10.1038/nphoton.2007.171.
[30] M. P. Nezhad, A. Simic, O. Bondarenko, et al., "Room-temperature subwavelength metallo-dielectric lasers," *Nat. Photon.*, vol. 4, pp. 395–399, 2010, https://doi.org/10.1038/nphoton.2010.88.
[31] C. Y. Lu, S. W. Chang, S. L. Chuang, T. D. Germann, D. Bimberg, "CW substrate-free metal-cavity surface microemitters at 300 K," Appl. Phys. Lett., vol. 96, Art no. 251101, 2010, https://doi.org/10.1088/0268-1242/26/1/014012.
[32] M. W. Kim, P. C. Ku, "Lasing in a metal-clad microring resonator," *Appl. Phys. Lett.* 2011, vol. 98, Art no. 131107, https://doi.org/10.1063/1.3573818.
[33] K. Ding, Z. C. Liu, L. J. Yin, et al., "Room-temperature continuous wave lasing in deep-subwavelength metallic cavities under electrical injection," *Phys. Rev. B* 2012, vol. 85, Art no. 041301, https://doi.org/10.1103/physrevb.85.041301.
[34] K. Ding, L. Yin, M. T. Hill, Z. Liu, P. J. van Veldhoven, C. Z. Ning, "An electrical injection metallic cavity nanolaser with azimuthal polarization," *Appl. Phys. Lett.*, vol. 102, Art no. 041110, 2013, https://doi.org/10.1063/1.4775803.
[35] K. Ding, M. T. Hill, Z. C. Liu, L. J. Yin, P. J. van Veldhoven, C. Z. Ning, "Record performance of electrical injection sub-wavelength metallic-cavity semiconductor lasers at room temperature," *Opt. Express*, vol. 21, pp. 4728–4733, 2013, https://doi.org/10.1364/oe.21.004728.

[36] Q. Gu, J. Shane, F. Vallini, et al., "Amorphous Al_2O_3 Shield for thermal management in electrically pumped metallo-dielectric nanolasers," *IEEE J. Quant. Electron.*, vol. 50, pp. 499–509, 2014, https://doi.org/10.1109/jqe.2014.2321746.
[37] S. H. Pan, Q. Gu, A. E. Amili, F. Vallini, Y. Fainman, "Dynamic hysteresis in a coherent high-β nanolaser," *Optica*, vol. 3, pp. 1260–1265, 2016, https://doi.org/10.1364/OPTICA.3.001260.
[38] M. A. Noginov, G. Zhu, A. M. Belgrave, et al., "Demonstration of a spaser-based nanolaser," *Nature*, vol. 460, pp. 1110–1112, 2009, https://doi.org/10.1038/Nature08318.
[39] X. G. Meng, A. V. Kildishev, K. Fujita, K. Tanaka, V. M. Shalaev, "Wavelength-tunable spasing in the visible," *Nano Lett.*, vol. 13, pp. 4106–4112, 2013, https://doi.org/10.1021/nl4015827.
[40] C. Zhang, Y. Lu, Y. Ni, et al., "Plasmonic lasing of nanocavity embedding in metallic nanoantenna array," *Nano Lett.*, vol. 15, pp. 1382–1387, 2015, https://doi.org/10.1021/nl504689s.
[41] E. I. Galanzha, R. Weingold, D. A. Nedosekin, et al., "Spaser as a biological probe," *Nat. Commun.*, vol. 8, pp. 15528, 2017, https://doi.org/10.1038/ncomms15528.
[42] K. Yu, A. Lakhani, M. C. Wu, "Subwavelength metal-optic semiconductor nanopatch lasers," *Opt. Express*, vol. 18, pp. 8790–8799, 2010, https://doi.org/10.1364/oe.18.008790.
[43] A. M. Lakhani, M. K. Kim, E. K. Lau, M. C. Wu, "Plasmonic crystal defect nanolaser," *Opt. Express*, vol. 19, pp. 18237–18245, 2011, https://doi.org/10.1364/oe.19.018237.
[44] E. K. Keshmarzi, R. N. Tait, P. Berini, "Single-mode surface plasmon distributed feedback lasers," *Nanoscale*, vol. 10, pp. 5914–5922, 2018, https://doi.org/10.1039/c7nr09183d.
[45] P. J. Cheng, Z. T. Huang, J. H. Li, et al., "High-performance plasmonic nanolasers with a nanotrench defect cavity for sensing applications," *ACS Photonics* 2018, vol. 5, pp. 2638–2644, https://doi.org/10.1021/acsphotonics.8b00337.
[46] M. Khajavikhan, A. Simic, M. Katz, et al., "Thresholdless nanoscale coaxial lasers," *Nature*, vol. 482, pp. 204–207, 2012, https://doi.org/10.1038/Nature10840.
[47] W. E. Hayenga, H. G. Gracia, H. Hodaei, et al. "Second-order coherence properties of metallic nanolasers," *Optica*, vol. 3, pp. 1187–1193, 2016, https://doi.org/10.1364/OPTICA.3.001187.
[48] Ma R. M., Yin X. B., Oulton R. F., Sorger V. J., Zhang X., "Multiplexed and electrically modulated plasmon laser circuit," *Nano Lett.*, 12, 5396–5402, 2012, https://doi.org/10.1021/nl302809a.
[49] Y. H. Chou, K. B. Hong, C. T. Chang, et al., "Ultracompact pseudowedge plasmonic lasers and laser arrays," *Nano Lett.*, vol. 18, pp. 747–753, 2018, https://doi.org/10.1021/acs.nanolett.7b03956.
[50] K. C. Shen, C. T. Ku, C. Hsieh, H. C. Kuo, Y. J. Cheng, D. P. Tsai, "Deep-ultraviolet hyperbolic metacavity laser," *Adv. Mater*, vol. 30, pp. 1706918, 2018, https://doi.org/10.1002/adma.201706918.
[51] W. Zhou, M. Dridi, J. Y. Suh, et al., "Lasing action in strongly coupled plasmonic nanocavity arrays," *Nat. Nanotechnol.*, vol. 8, pp. 506–511, 2013, https://doi.org/10.1038/nnano.2013.99.
[52] F. van Beijnum, P. J. van Veldhoven, E. J. Geluk, et al., "Surface plasmon lasing observed in metal hole arrays," *Phys. Rev. Lett.*, vol. 110, Art no. 206802, 2013, https://doi.org/10.1103/physrevlett.110.206802.
[53] A. Yang, T. B. Hoang, M. Dridi, et al., "Real-time tunable lasing from plasmonic nanocavity arrays," *Nat. Commun.*, vol. 6, pp. 6939, 2015, https://doi.org/10.1038/ncomms7939.
[54] A. H. Schokker, A. F. Koenderink, "Lasing in quasi-periodic and aperiodic plasmon lattices," *Optica*, vol. 3, pp. 686–693, 2016, https://doi.org/10.1364/optica.3.000686.
[55] V. T. Tenner, M. J. A. de Dood, M. P. van Exter, "Measurement of the phase and intensity profile of surface plasmon laser emission," *ACS Photonics*, vol. 3, pp. 942–946, 2016, https://doi.org/10.1021/acsphotonics.6b00239.
[56] D. Wang, A. Yang, W. Wang, et al., "Band-edge engineering for controlled multi-modal nanolasing in plasmonic superlattices," *Nat. Nanotechnol.*, vol. 12, pp. 889–894, 2017, https://doi.org/10.1038/nnano.2017.126.
[57] D. Wang, M. R. Bourgeois, W. K. Lee, et al., "Stretchable nanolasing from hybrid quadrupole plasmons," *Nano Lett.*, vol. 18, pp. 4549–4555, 2018, https://doi.org/10.1021/acs.nanolett.8b01774.
[58] A. Fernandez-Bravo, D. Wang, E. S. Barnard, et al., "Ultralow-threshold, continuous-wave upconverting lasing from subwavelength plasmons," *Nat. Mater.*, vol. 18, pp. 1172–1176, 2019, https://doi.org/10.1038/s41563-019-0482-5.
[59] Ma R. M., Oulton R. F., "Applications of nanolasers," *Nat. Nanotechnol.*, vol. 14, pp. 12–22, 2019, https://doi.org/10.1038/s41565-018-0320-y.
[60] M. A. Noginov, J. B. Khurgin, "Miniature lasers: Is metal a friend or foe?" *Nat. Mater.*, vol. 17, pp. 116–117, 2018, https://doi.org/10.1038/nmat5065.
[61] R. M. Ma, "Lasing under ultralow pumping," *Nat. Mater.*, vol. 18, pp. 1152–1153, 2019, https://doi.org/10.1038/s41563-019-0513-2.
[62] S. Wang, H. Z. Chen, R. M. Ma, "High performance plasmonic nanolasers with external quantum efficiency exceeding 10%," *Nano Lett.*, vol. 18, pp. 7942–7948, 2018, https://doi.org/10.1021/acs.nanolett.8b03890.
[63] R. M. Ma, X. Yin, R. F. Oulton, V. J. Sorger, X. Zhang, "Multiplexed and electrically modulated plasmon laser circuit," *Nano Lett.*, vol. 12, pp. 5396–5402, 2012, https://doi.org/10.1021/nl302809a.
[64] T. Keating, S. H. Park, J. Minch, et al., "Optical gain measurements based on fundamental properties and comparison with many-body theory," *J. Appl. Phys.*, vol. 86, pp. 2945–2952, 1999, https://doi.org/10.1063/1.371153.
[65] A. Einstein, "Zur quantentheorie der strahlung," *Phys Z*, vol. 18, pp. 121–128, 1917.